

## Covalent-like Interactions between Artificial Atoms inside Silver Supercrystals

Xun Wang,\* Jing Zhuang, Ziyang Huo, Shi Hu, and Yadong Li

Department of Chemistry, Tsinghua University, Beijing 100084, P. R. China

Received September 13, 2007

In this paper, a description of the process by which two kinds of surfactants with relative long or short alkyl chains are introduced onto the surface of Ag nanocrystals, which contribute to the formation of tunable and anisotropic “covalent bonds” between two Ag nanocrystals, is given. By altering the lengths of the short alkyl chains, the sizes and structures of the as-obtained supercrystals as well as the exposed crystal planes of the interior nanocrystals can be tuned. This strategy may further enrich the “chemical bond” categories of artificial atoms and serve as the base for the discovery of more functional superstructures.

### Introduction

Monodisperse nanocrystals with controlled size, shape, and properties have been utilized as artificial atoms to built all kinds of two-dimensional or three-dimensional superlattice structures via self-assembly processes.<sup>1–12</sup> While real atoms combine with others via ionic, metallic, or covalent bonds, these artificial atoms interact with each other via Coulombic, charge–dipole, dipole–dipole, dispersive (van der Waals), or dipolar interactions of nonlocal dipoles.<sup>13–17</sup> Since most

of these interactions are isotropic, these artificial atoms have always been treated as hard spheres when constructing complex superstructures, which may limit the exploration of the phase variety of superlattice structures. In this paper, a description of the process by which two kinds of surfactants with relative long or short alkyl chains are introduced onto the surface of Ag nanocrystals, which contribute to the formation of tunable and anisotropic “covalent bonds”<sup>18</sup> between two Ag nanocrystals, is given. By altering the lengths of the short alkyl chains, the sizes and structures of the as-obtained supercrystals as well as the exposed crystal planes of the interior nanocrystals can be tuned. This strategy may further enrich the “chemical bond” categories of artificial atoms and serve as the basis for the discovery of more functional superstructures.

The difference in chemical bonding between atoms with different diameters results in various long-range spatial distributions of atoms in crystals. In a similar way, the interaction between the artificial atom units of the superstructures would be key for the discovery of their assembly behavior. Our initial aim is to mimic the electron structure of the real atoms, which leads to the formation of anisotropic covalent bonds via the sharing of electrons. Fatty acids or amines with long alkyl chains have been widely used as

\* To whom correspondence should be addressed. E-mail: wangxun@mail.tsinghua.edu.cn.

- (1) Sastry, M.; Rao, M.; Ganesh, K. N. *Acc. Chem. Res.* **2002**, *35*, 847.
- (2) Murray, C. B.; Kagan, C. R.; Bawendi, M. G. *Science* **1995**, *270*, 1335.
- (3) Shenton, W.; Pum, D.; Sleytr, U. B.; Mann, S. *Nature* **1997**, *389*, 585.
- (4) Sun, S. H.; Murray, C. B.; Weller, D.; Folks, L.; Moser, A. *Science* **2000**, *287*, 1989.
- (5) Kim, F.; Kwan, S.; Akana, J.; Yang, P. D. *J. Am. Chem. Soc.* **2001**, *123*, 4360.
- (6) Yang, P. D. *Nature* **2003**, *425*, 243.
- (7) Velikov, K. P.; Christova, C. G.; Dullens, R. P. A.; van Blaaderen, A. *Science* **2002**, *296*, 106.
- (8) Zeng, H.; Li, J.; Liu, J. P.; Wang, Z. L.; Sun, S. H. *Nature* **2002**, *420*, 395.
- (9) Tang, Z. Y.; Zhang, Z. L.; Wang, Y.; Glotzer, S. C.; Kotov, N. A. *Science* **2006**, *314*, 274.
- (10) Yang, Y.; Liu, S. M.; Kimura, K. *Angew. Chem., Int. Ed.* **2006**, *45*, 5662.
- (11) Wang, X.; Zhuang, J.; Peng, Q.; Li, Y. D. *Nature* **2005**, *437*, 121.
- (12) Wang, X.; Peng, Q.; Li, Y. D. *Acc. Chem. Res.* **2007**, *40*, 635.
- (13) Kalsin, A. M.; Fialkowski, M.; Paszewski, M.; Smoukov, S. K.; Bishop, K. J. M.; Grzybowski, B. A. *Science* **2006**, *310*, 420.
- (14) Shevchenko, E. V.; Talapin, D. V.; Kotov, N. A.; O'Brien, S.; Murray, C. B. *Nature* **2006**, *439*, 55.
- (15) (a) Kalsin, A. M.; Pinchuk, A. O.; Smoukov, S. K.; Paszewski, M.; Schatz, G. C.; Grzybowski, B. A. *Nano Lett.* **2006**, *6*, 1896. (b) Kalsin, A. M.; Grzybowski, B. A. *Nano Lett.* **2007**, *7*, 1018.

- (16) Talapin, D. V.; Shevchenko, E. V.; Murray, C. B.; Titov, A. V.; Král, P. *Nano Lett.* **2007**, *7*, 1213.
- (17) Bolhuis, P. G.; Frenkel, D.; Mau, S. C.; Huse, D. A. *Nature* **1997**, *388*, 235.
- (18) (a) DeVries, G. A.; Brunnbauer, M.; Hu, Y.; Jackson, A. M.; Long, B.; Neltner, B. T.; Uzun, O.; Wunsch, B. H.; Stellacci, F. *Science* **2007**, *315*, 358. (b) Perepichka, D. F.; Rosei, F. *Angew. Chem., Int. Ed.* **2007**, *46*, 6006. (c) Kiely, C. J.; Fink, J.; Brust, M.; Bethell, D.; Schiffrin, D. J. *Nature* **1998**, *396*, 444.

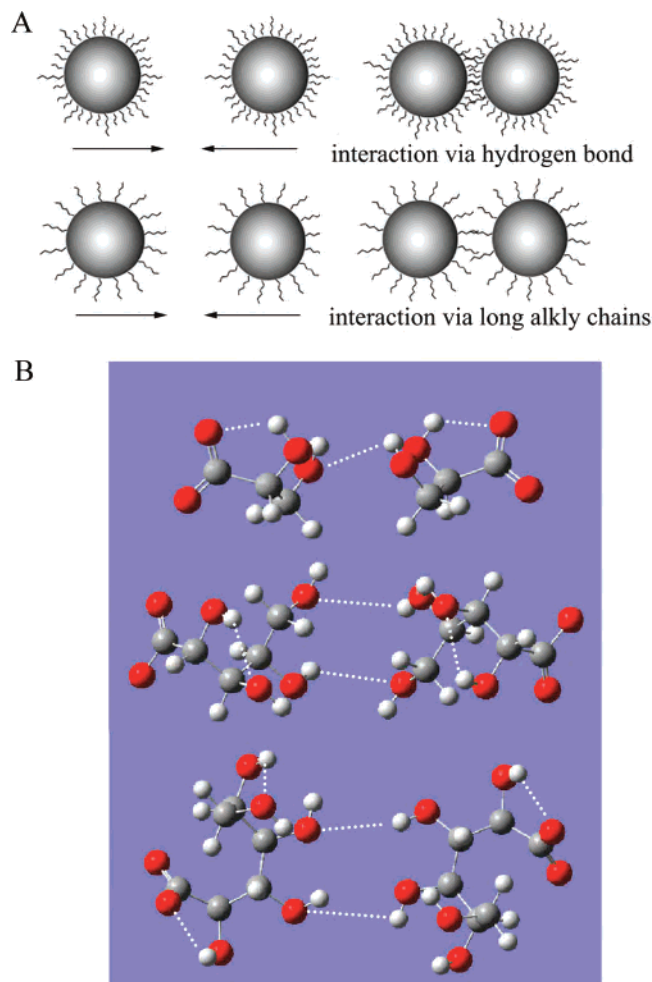


**Figure 1.** (A) Illustration of the interaction modes between two nanocrystals covered with only long alkyl chains (bottom) or long–short alkyl chains (top). (B) Interaction between two saccharate molecules. From bottom to top: gluconic acid (6C), arabonic acid (5C), and dihydroxypropionic acid (3C). Color key: gray balls, carbon atoms; red balls, oxygen; white balls, hydrogen; dotted lines, hydrogen bonds.

protecting reagents for the stabilization of monodisperse nanocrystals. While the overlap contacts of the alkyl chains have been shown to play an important role in the self-assembly process of monodisperse nanocrystals, their lengths (about 1.7 nm) prevent true and close contact between the nanocrystals.<sup>19,20</sup> Following this contact mode, these artificial atoms are reasonably treated as hard spheres with their shape and structure uninfluenced. So the first thing to do to realize true and close contact is to bring the nanocrystals closer. It was imagined that if some shorter alkyl chains with hydroxyl groups were fixed onto the surface of the nanocrystals, the interaction between long alkyl chains would first bring the nanocrystals to a distance of about 1~2 nm, and then the short alkyl chains with hydroxyl groups would interact with each other and bring the nanocrystals much closer (Figure 1A). In analogy to the radial distribution of s and p electron clouds in real atoms, the short and long alkyl chains of the artificial atoms would contribute to the formation of “covalent bonds”. Wide-angle X-ray diffraction (XRD) patterns

(19) Huo, Z. Y.; Chen, C.; Li, Y. D. *Chem. Commun.* **2006**, 3522.

(20) Wang, X.; Li, Y. D. *Chem. Commun.* **2007**, 2901.

(21) Donkers, R. L.; Lee, D.; Murray, R. W. *Langmuir* **2004**, *20*, 1945.

taken from these supercrystals samples show that the interaction between the artificial atoms should be anisotropic.

## Experimental Section

We have chosen oleic acid and octadecylamine as the long alkyl chains and saccharate (saccharate was formed via the in-situ oxidation of the monosaccharide by  $\text{Ag}^+$  ions) as the short alkyl chains with hydroxyl groups. While the length of the long alkyl chains was fixed as 18 C atoms, the length of the short alkyl chains was changed from 3 and 5 to 6 C atoms (Figure 1B). Considering that monosaccharides are usually classified as D or L type, different types of monosaccharide were adopted in our experiments, including D-glucose (6C-D), L-glucose (6C-L), D-arabinose (5C-D), L-arabinose (5C-L), and D, L-glyceraldehyde (3C-D, L).

Our synthesis was based on a modified liquid–solid–solution strategy.<sup>11</sup> In a typical synthesis, 0.5 g of octadecylamine, 4 mL of oleic acid, and 16 mL of ethanol were mixed together under agitation to form solution A; 0.4 g of  $\text{AgNO}_3$  and 1 g of monosaccharide (for example, 6C-D, 6C-L, 5C-D, 5C-L, and 3C-D, L) were dissolved into 15 mL of distilled water, to which 2 mL of  $\text{NH}_3\text{H}_2\text{O}$  (6 mol/L) was added to form solution B; solution B was mixed with solution A under agitation, then transferred to a 40 mL autoclave, sealed, and hydrothermally treated at the designated temperature of 100 °C for about 1.5 h. After the autoclave was cooled to room temperature, the product was obtained in the form of a dark-brown homogeneous suspension (about 35 mL in volume). In order to obtain colloidal superstructures, 20 mL of the as-obtained solution was added dropwise to a mixed solution of 50 mL of cyclohexane, 25 mL of ethanol and 15 mL of distilled water under agitation. After aging for about 3 h, the mixture will separate into two phases, and the organic colloidal phase containing silver superstructures can be collected with a separating funnel. These supercrystals can be precipitated by adding excess amount of ethanol to the solution or be separated by slow evaporation of the solvents. The obtained sample was characterized on a Bruker D8-Avance X-ray powder diffractometer with Cu K $\alpha$  radiation ( $\lambda = 1.5418 \text{ \AA}$ ). The size and morphology of the nanocrystals were determined by a JEOL JEM-1200EX transmission electron microscope (TEM) at 100 kV and a Tecnai G2 F20 S-Twin high-resolution transmission electron microscope (HRTEM) at 200 kV.

## Results and Discussion

A facile strategy was first developed to assembly these Ag nanocrystals into three-dimensional supercrystals. Since ethanol is a poor solvent and cyclohexane is a good solvent for nanocrystals covered with alkyl chains, Ag supercrystals were obtained by tuning the ratio of ethanol and cyclohexane to about 1:2. A reversible dissolution–deposition process of Ag nanocrystals upon the surface of supercrystals will facilitate the formation of perfect supercrystals with highly ordered inner structures, similar to those of ions in a colloidal solution. With the increase in the concentration of the Ag nanocrystals, the growth of supercrystals will undergo a process similar to the “Lamar process” in real crystal growth, including a burst of nucleation stage and a gradual growth stage (Figure 2). The colloidal solution of silver supercrystals was transparent, and no phase separation occurred even after several months, indicating that it was thermodynamic stable like a colloidal solution. Experimental results showed that the length of the short alkyl chains played an important role

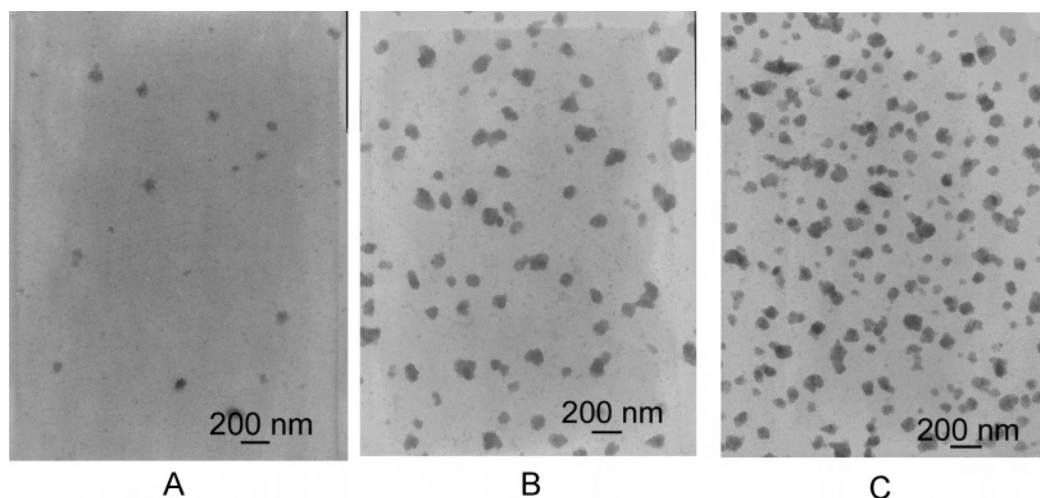


**Figure 2.** Formation process of Ag supercrystals with the addition of 6C-modified nanocrystal solution into the system: (A) 0.0123 mol/L Ag nanocrystals; (B) 0.0137 mol/L Ag nanocrystals; and (C) 0.0163 mol/L Ag nanocrystals.

in the formation of these supercrystals. Before the assembly processes, the nanocrystals obtained through reduction of  $\text{Ag}^+$  by 6C-D, 6C-L, 5C-D, 5C, L, and 3C-D, L had nearly the same diameters of about 5 nm (Figure 3A1 inset and Figure 3B1 inset), which ensured that these building blocks were only different in the long–short protecting reagents. Under the same conditions, the diameters of the colloidal particles were in the range of 150–200 nm for 6C-modified supercrystals (Figure 3A1), 180–300 nm for 5C-modified supercrystals (Figure 3B1), and 300–400 nm for 3C-modified supercrystals (Figure 3C1). It was apparent that with the changing of the lengths of the short alkyl chains, the sizes of supercrystals were changed. No apparent difference in sizes was observed between the D- and L-type saccharate with the same alkyl chains.

The TEM characterization showed that the 6C-D or 6C-L supercrystal samples were composed of large quantity of particles with sizes in the range of 150–200 nm (Figure 3A). TEM images with higher resolution indicated that they were indeed composed of uniform nanocrystals (Figure 3A2). HRTEM characterizations showed that each nanocrystal was a single crystal. The size of these nanocrystals did not change before or after the assembly process; however, the shape of Ag nanocrystals was distorted to some extent. The distance between two adjacent Ag nanocrystals can be measured to be less than 0.5 nm, and most of them shared a common region and connected to each other directly (Figure 3A3,–A4), a case similar to the formation of covalent bonds between two atoms. Compared with the two-dimensional arrays on the TEM grids (the distance between two nanocrystals is about 2.5 nm, Figure 3A1 inset), stronger interaction must exist inside these supercrystals. Careful observations indicated that most of these nanocrystals crystallized in face-centered-cubic (fcc) structures, which were further confirmed by the following small-angle XRD results (Figure 3D)  $d$  values of 8.6, 6.1, and 5.2 nm can be indexed to the (111), (200), and (220) planes of fcc crystal structure).

When the lengths of the short alkyl chains were reduced from six to five (the 5C-D- or 5C-L-modified supercrystals), the interaction between nanocrystals would be tuned to some

extent (calculation value). Besides the change in size from 150–200 to 180–300 nm, HRTEM characterization on their interior structures showed that the nanocrystals were even distorted into near-cubic shapes (Figure 3B3), indicating that stronger interaction between two adjacent nanocrystals has led to a surface reconstruction process of the interior nanocrystals. This shape transformation led to a new structure of simple cubic piling modes for the nanocrystals, in which each nanocrystal touches six neighbors. Fast Fourier transform (FFT) patterns of the supercrystals confirmed this piling mode (Figure 3B4). Small-angle XRD results coincided well with TEM observation, and the main peaks at 7.9, 5.6, and 3.9 nm can be indexed to the (110), (200), and (220) planes of simple cubic structure (Figure 3D). In case of 3C-D, L-modified supercrystals, TEM characterization showed that the sizes are apparently larger than the 6C- and 5C-modified ones. fcc structures and piling modes similar to those of 6C-modified ones were observed for the 3C-modified supercrystals (Figure 3D).

Wide-angle XRD results provided us further information on the overall structures and nanocrystal contacting modes inside the macro supercrystal samples. As shown in Figure 4A, the XRD patterns for the 6C-L-modified nanocrystals without formation of supercrystals show the characteristic three peaks of (111), (200), and (220) of fcc-structured Ag (space group,  $Fm\bar{3}m$  (225)) with lattice constants of  $a = 4.0862$  nm (JCPDS 4-783). The diffraction peaks in the XRD patterns are apparently broadened compared with those of the bulky ones due to the nanosized diameters. With the formation of supercrystals, it was observed that the (200) and (220) peaks disappeared and only that of (111) was preserved in the XRD patterns. A controlled experiment was carried out by dissolving the supercrystals into monodisperse nanocrystals with an excess of cyclohexane; the (200) and (220) peaks in the XRD patterns were then recovered. This might indicate that inside the supercrystals, the interaction between two Ag nanocrystals was anisotropic, and only interaction along  $\langle 100 \rangle$  or  $\langle 110 \rangle$  was allowed. This contacting mode left aside the (111) planes when forming supercrystals. Similar results were observed for the 3C-



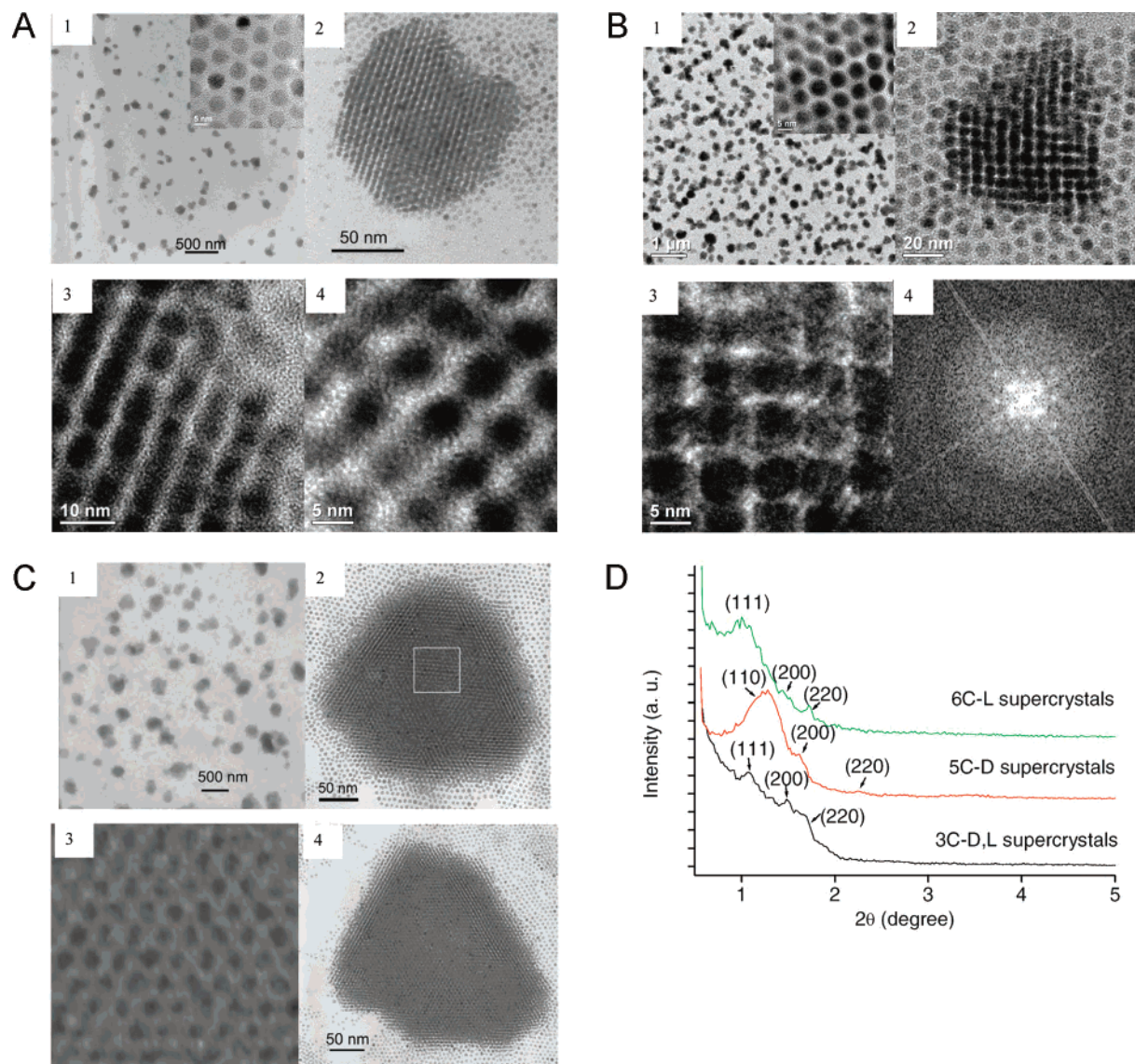


**Figure 3.** (A) 1–4, TEM images of 6C-L-modified supercrystals; 1 inset, monodisperse 6C-L-modified nanocrystals before assembly. (B) 1–3, TEM images of 5C-L-modified supercrystals; 1 inset, monodisperse 5C-L-modified nanocrystals before assembly; 4, FFT of Figure 2B3. (C) 1, TEM images of 3C-D, L-modified supercrystals; 2–4, individual fcc 3C-D, L-modified supercrystal, along [111] directions. (D) Small-angle XRD patterns for the 6C-L-, 5C-D-, and 3C-D, L-modified supercrystals.

modified supercrystals. Wide-angle XRD characterization showed that only the (111) peak existed, and (200) and (220) were apparently reduced (Figure 4B). This result further confirmed that the 6C- and 3C-modified supercrystals have the same crystal structure and piling modes.

Wide-angle XRD patterns of 5C-D- and 5C-L-modified supercrystals showed that all the peaks of (111), (200), and (220) exist (Figure 4B). On the basis of the TEM characterization, these 5C-modified nanocrystals distorted into nearly cubic-shaped nanocrystals, the surface of which were dominated with (111), (100), and (110), and these three characteristic peaks were exposed in simple cubic piling modes. These results also proved that the interaction directions for two close nanocrystals were along  $\langle 100 \rangle$ . All our experimental results showed that the interaction between two adjacent Ag nanocrystals could be anisotropic, one of the most important features of covalent bonds.

The disappearance or weakening of diffraction peaks in XRD patterns was usually observed in the controlled synthesis of nanocrystals with different shapes.<sup>22–26</sup> For example, only (111) planes exist in the XRD patterns of Ag nanocrystals with triangular plate shapes,<sup>25</sup> and the intensities of (200) were much stronger than those of (111) in cubic-shaped Ag nanocrystals.<sup>26</sup> In current studies, since these supercrystals were assembled from spherical nanocrystals, the disappearance of the (200) and (220) peaks in the XRD patterns can only be attributed to the anisotropic interaction

(22) Kim, F.; Connor, S.; Song, H.; Kuykendall, T.; Yang, P. D. *Angew. Chem., Int. Ed.* **2004**, *43*, 3673.

(23) Sun, Y. G.; Xia, Y. N. *Science* **2002**, *298*, 2176.

(24) Xiong, Y. J.; McLellan, J. M.; Chen, J. Y.; Yin, Y. D.; Li, Z. Y.; Xia, Y. N. *J. Am. Chem. Soc.* **2005**, *127*, 17118.

(25) Zhang, J. T.; Li, X. L.; Sun, X. M.; Li, Y. D. *J. Phys. Chem. B* **2005**, *109*, 12544.

(26) Xu, R.; Wang, D. S.; Zhang, J. T.; Li, Y. D. *Chem. Asian J.* **2006**, *1*, 888–893.

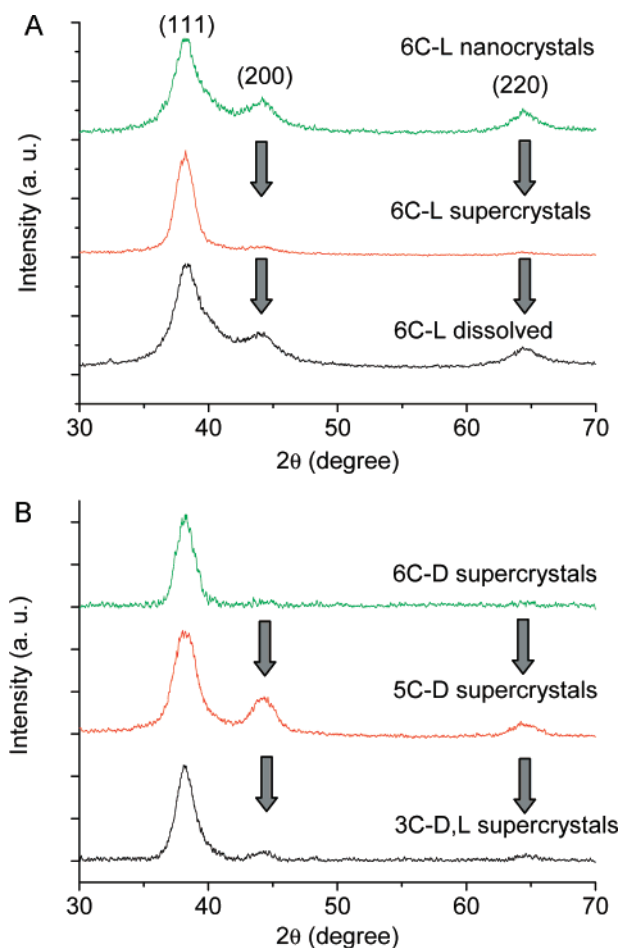


**Figure 4.** (A) Wide-angle XRD patterns for 6C-L-modified nanocrystals before assembly, 6C-L supercrystals, and 6C-L-modified nanocrystals obtained via dissolving the supercrystals. (B) Wide-angle XRD patterns for 6C-D-, 5C-D-, and 3C-D, L-modified supercrystals.

between the interior artificial atoms, which may be induced by the selective adsorption of different surfactants on different crystal planes.

The self-assembly of nanocrystals into two- or three-dimensional superlattices is a very complicated process. So far the driving forces for these process can be classified as those of enthalpy-driven, dipole–dipole interactions, or electrostatic, etc., which have been investigated and proven to govern the assembly process of monodisperse nanocrystals. However, it is most possible that these forces work simultaneously during the self-assembly process. One driving force may play a more important role when it is greater than that of the others. In this case, it is also reasonable to emphasize one of these driving forces when others are fixed. In our work, we found that while the residual charge present on the nanoparticles played an important role in the formation of Ag supercrystals (Supporting Information Section 4), the short–long alkyl chains absorbed on the surface of the nanocrystals would lead to anisotropic interaction between nanocrystals, which was confirmed by the wide-angle XRD characterization of these nanocrystals. Since the electrostatic force can theoretically only lead to isotropic interaction, the influence of residual charge on the surface of nanocrystals has been omitted.

FTIR spectra taken from the supercrystal powder samples clearly showed the coexistence of  $\text{COO}^-$  and  $\text{OH}^-$  groups on the supercrystals (Supporting Information Figures 1–3), proving that the long and short alkyl chain ligands were absorbed on the surface of the nanocrystals.  $^1\text{H}$  NMR spectra (Supporting Information Figures 4–6) taken from the colloidal solution of supercrystals showed broadened peaks compared with those of free ligands, indicating that most of the ligands in the system were absorbed on the surface of the supercrystals or the inner nanocrystals<sup>21</sup> so that the influence of free ligands on the assembly process can be neglected. On the basis of the TEM observation, the nanocrystals modified with long–short alkyl chains interacted and combined with other nanocrystals via the sharing of a common region. For 5C-modified ones, the nanocrystals even self-adjust into nearly cubic shapes to obtain closer contact. Calculations (Supporting Information) on the interaction between two 5C saccharates indicated that their overlap would lower the energy of the system by  $-57.139056$  kJ/mol because of the formation of hydrogen bonds. On the basis of our experimental results, the subsequent surface reconstruction process would occur when the nanocrystals were brought closer, which might lead to different piling modes. It is worthy to note that the radial length of 6C is even shorter than that of 5C because of the formation of the intramolecular hydrogen bond in the 6C saccharate molecule (Figure 1B). This may be the reason why the 6C- and 3C-modified supercrystals have the same crystal structure and piling modes of close-packed fcc while 5C-modified ones have simple cubic structures.

## Conclusion

In this paper, a new strategy was developed to realize the “covalent bonds” between two artificial atoms inside silver supercrystals. By tuning the lengths of the short alkyl chains, the sizes and structures of the as-obtained supercrystals as well as the exposed crystal planes of the interior nanocrystals can be tuned. This study shows the possibility of tuning the “chemical bonds” between two artificial atoms in a fashion such as that done with real atoms, which may lead to the discovery of new types of porous noble-metal catalysts for structure-sensitive catalytic processes.

**Acknowledgment.** This work was supported by the NSFC (20725102, 50772056), the Foundation for the Author of National Excellent Doctoral Dissertation of P. R. China, the Program for New Century Excellent Talents of the Chinese Ministry of Education, and the State Key Project of Fundamental Research for Nanoscience and Nanotechnology (2006CB932300).

**Supporting Information Available:** Calculations on the interaction between two 5C saccharates; FTIR spectra; NMR spectra; in PDF format. This material is available free of charge via the Internet at <http://pubs.acs.org>.

IC701811F